The sea–air exchange of mercury (Hg) in the marine boundary layer of the Augusta basin (southern Italy): Concentrations and evasion flux

E. Bagnato [a,*], M. Sproveri [b], M. Barra [c], M. Bitetto [a], M. Bonsignore [b], S. Calabrese [a], V. Di Stefano [b], E. Oliveri [b], F. Parello [a], S. Mazzola [c]

[a] DiSTeM, University of Palermo, Via Archirafi 36, 90123 Palermo, Italy
[b] IAMC-CNR, Capo Granitola, Via del Mare 3, 91021 Torretta Granitola, Trapani, Italy
[c] IAMC-CNR, Naples, Calata Porta di Massa, Naples, Italy

HIGHLIGHTS

- The Hg evasion flux in the Augusta basin marine boundary layer was examined.
- The human activity has influenced in the past the marine Hg cycle in the Augusta Bay.
- The release of Hg from the Augusta Bay is a source of pollution for the Mediterranean.

ARTICLE INFO

ABSTRACT

The first attempt to systematically investigate the atmospheric mercury (Hg) in the MBL of the Augusta basin (SE Sicily, Italy) has been undertaken. In the past the basin was the receptor for Hg from an intense industrial activity which contaminated the bottom sediments of the Bay, making this area a potential source of pollution for the surrounding Mediterranean. Three oceanographic cruises have been thus performed in the basin during the winter and summer 2011/2012, where we estimated averaged Hg_{atm} concentrations of about 1.5 ± 0.4 (range 0.9–3.1) and 2.1 ± 0.98 (range 1.1–3.1) ng m^{-3} for the two seasons, respectively. These data are somewhat higher than the background Hg_{atm} value measured over the land (range 1.1 ± 0.3 ng m^{-3}) at downtown Augusta, while are similar to those detected in other polluted regions elsewhere. Hg evasion fluxes estimated at the sea/air interface over the Bay range from 3.6 ± 0.3 (unpolluted site) to 72 ± 0.1 (polluted site of the basin) ng m^{-2} h^{-1}. By extending these measurements to the entire area of the Augusta basin ($\sim$23.5 km^2), we calculated a total sea–air Hg evasion flux of about 9.7 ± 0.1 g d^{-1} ($\sim$0.004 t yr^{-1}), accounting for $\sim$0.0002% of the global Hg oceanic evasion (2000 t yr^{-1}). The new proposed data set offers a unique and original study on the potential outflow of Hg from the sea–air interface at the basin, and it represents an important step for a better comprehension of the processes occurring in the marine biogeochemical cycle of this element.

© 2013 Elsevier Ltd. All rights reserved.

1. Introduction

Mercury (Hg) is a chronic pollutant of global concern known to be transported long distances in the atmosphere into remote ecosystems (Schroeder and Munthe, 1998). Hg flux into the atmosphere from natural and anthropogenic sources has been reviewed recently and new estimates for the worldwide distribution of anthropogenic emissions have been published (Pacyna and Pacyna, 1998; Kim et al., 2005; Travnikov, 2005; Amos et al., 2012). Although a part of the Hg emitted naturally comes from geological and geothermal sources, much of it is recycled Hg previously emitted from primary or anthropogenic sources, and subsequently re-deposited to terrestrial and ocean surfaces (Ericksen et al., 2005). Hence, as a consequence, a large part of the 2000 t of yearly emissions from natural sources is actually reemission of previously deposited mercury, much of which has an anthropogenic origin. In some instances, it has been discovered that marine sediments contaminated by industrial effluents may be secondary sources of Hg to aquatic ecosystems even though discharge has been strongly reduced or has even ceased (Bothner et al., 1980). The exchange of Hg between oceanic surfaces and the atmosphere represents an important process for the atmospheric cycling and environmental turnover of this element (Mason et al., 1994; Lam-

borg et al., 1999). The ability of GEM to reemit from terrestrial and aquatic surfaces keeps this element circulating in the environment, with burial into ocean sediments as the only long term sink. According to the global model of Hg biogeochemistry proposed by Mason et al. (1994), the ocean releases about 1/3 of the total global Hg emissions to the atmosphere (about 30% of the total budget of atmospheric mercury on a global scale) and receives about 30–70% of the global atmospheric deposition (Lamborg et al., 2002). Re-emissions from the ocean of previously deposited Hg are dominated by gaseous elemental mercury (Hg^0 or GEM ~ 2000 t yr^{-1}; Mason et al., 1994), the most volatile and long-lived form of this metal. Its low solubility and high Henry's Law constant induce high GEM evasion fluxes from fresh water systems, accounting for about 7–95% of the total estimated atmospheric Hg deposition in that system. By these considerations, currently there is a clear intent to increase both qualitative and quantitative knowledge concerning the processes occurring during the exchange of Hg between sediments, the overlying water column and sea-air interface. Within the frame of the IAMC-CNR/ASP program founded by the Regional Health Department of Syracuse, we performed a short-term (1 yr) monitoring study on Hg distribution and evasional flux in the atmospheric compartment of the Augusta basin (Fig. 1), a site of the Mediterranean Sea strongly affected in the past by the uncontrolled discharge of Hg (since the 1950s) from industrial and petrochemical plants (Sprovieri et al., 2011). This work represents an important step toward a better comprehension of the processes occurring once Hg is re-emitted from the contaminated bottom sediments (which actually represent the main source of Hg for the Bay; Sprovieri et al., 2011) in the water column and finally to the atmosphere. Although the water surface area of the Augusta basin represents only a small part of the total oceanic surfaces on Earth, we aimed this study may improve the global mercury budget and cycle which lack measurements in large parts of the world's marine environments. Our purposes are threefold: (1) to characterize the regional background level of atmospheric GEM as well as evasional fluxes of Hg in the Bay and compare with other areas at various latitudes; (2) to evaluate the regional sources (if any) eventually affecting the GEM_{atm} concentrations; and (3) to discuss the deposition of atmospheric Hg in the Augusta area. With these aims, a dynamic flux chamber coupled with a real-time atomic adsorption spectrometer (Lumex-RA 915+) has been used to measure Hg evasion flux at the sea/air interface during three intensive research oceanographic cruises performed in the winter and summer 2011–2012.

2. Methodology

2.1. Site location

The Augusta basin is within a natural Bay which occupies about 30 km of the eastern coast of the Sicily (Fig. 1a). The southernmost part of the basin hosted one of the most important chlor-alkali plants of Italy (Syndial Priolo Gargallo), which with 765 kg of Hg emission made up over 20% of total Italian emissions in 2001 (Le Donne and Ciafani, 2008). The effects of indiscriminate Hg discharge of the past include high Hg levels in bottom sediments which act as a source of Hg to the water column in the Augusta Bay (ICRAM, 2005; Sprovieri et al., 2011). In detail, sediments lying in the southern part of the Bay show the highest HgT levels (0.1–527.3 mg kg^{-1}) with a large range of variability (median value 23.8 mg kg^{-1}), while the northern area is characterized by sediments containing HgT concentrations varying from 0.1 to 12.7 mg kg^{-1} (median value 1.1 mg kg^{-1}) (Sprovieri et al., 2011). An averaged outflow of total Hg (HgT) from the Bay to the Augusta coastal waters has been estimated to be in the order of about 0.162 kmol yr^{-1} ($\sim$0.032 t yr^{-1}; Sprovieri et al., 2011), which corresponds to 1–2% of the amount calculated for the entire Mediterranean area (12.5 kmol yr^{-1}; Rajar et al., 2007). By these considerations it emerges that the Augusta basin may play an important role in exporting mercury into the Mediterranean Sea and represents a point source for that system.

2.2. Atmospheric GEM measurements

Measurements of atmospheric elemental gaseous mercury (GEM) were performed across the Augusta basin on-board the Italian CNR research vessel Luigi Sanzo, during three main oceanographic cruises carried out along the same route in the winter (November 2011) and summer (July 2011–June 2012) (Fig. 1b), chosen out of practical and logistical criteria. For the sake of simplicity, GEM, Hg and Hg^0 are used without distinction in this article, unless otherwise specified. The analysis of atmospheric GEM was performed using an automated real-time atomic adsorption
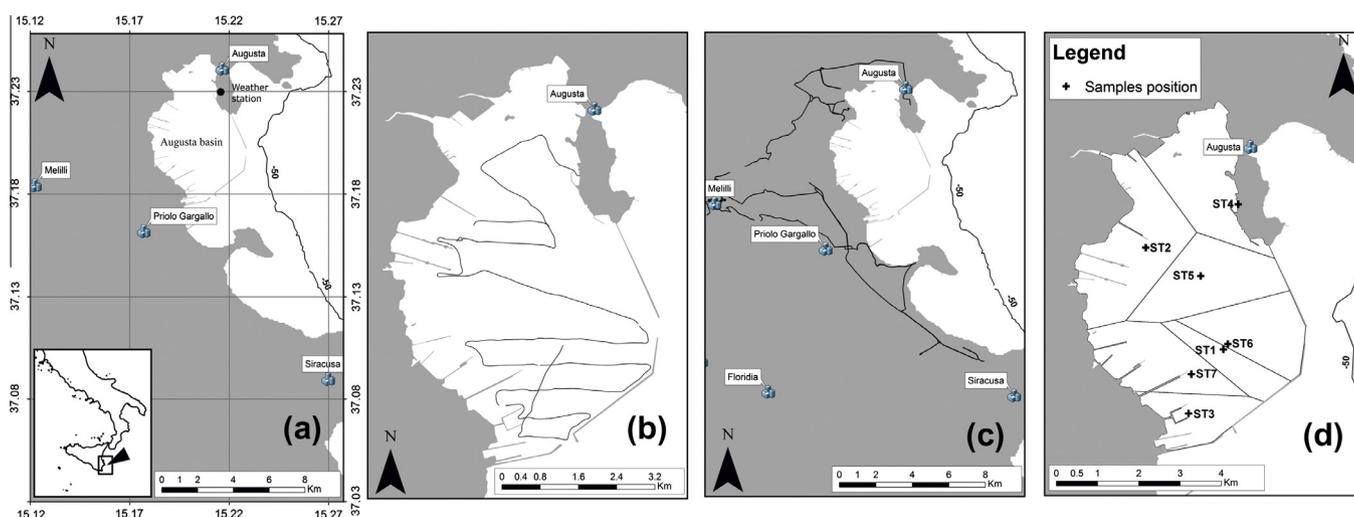

Fig. 1. Maps showing (a) the Augusta basin and the site of the installed weather station used in this study, (b) the routes of the oceanographic cruises inside the Augusta basin, (c) the land trajectories to detect GEM contents in the atmosphere along the coastal area, and (d) the stations for Hg evasion flux measurement by accumulation chamber technique (ST1–7). Map (c) also reports the partition of the entire basin into seven Voronoi polygons, each relative to one station of measurement (see text for detail).

spectrometer (Lumex-RA 915+). The Lumex sampled air at about 20 l min^{-1} directly into the instrument's sampling inlet ($\sim$3 cm diameter) at ambient temperature to the multi path detection cell which has an effective path length of 10 m. This multi-path cell has a volume of 0.7 l and air changes in the cell 3 times every 7–10 s. The instrument inlet has an external washable dust filter with a porosity of 5–10 mkm in addition to a coarse dust filter of porosity 100 mkm. The Lumex monitored gaseous elemental mercury (GEM) concentrations using differential atomic absorption spectrometry with correction for background absorption via the Zeeman Effect (Sholupov et al., 2004). A zero correction resets the baseline every 5 min during sampling. The detection limit was $\sim$2 ng m^{-3}, and the instrument has an accuracy of 20%. The accuracy and precision of the applied instrumentation has also been assessed through comparison with the traditional gold trap/CVAFS system used at remote sites elsewhere (Aiuppa et al., 2007; Witt et al., 2008). During the cruises, the air inlet of the analyzer was installed on the upper deck about 3 m a.s.l. to avoid the contamination from ship emissions. We sampled air at 1 s intervals by covering a total marine area of about 60 km at a speed of $\sim$10 km h^{-1}. Lumex has also been employed to measure atmospheric GEM concentration over the land along the shoreline surrounding the Augusta basin (Fig. 1c), in order to assess background Hg levels in the air masses inland. For this purpose, the inlet of the instrument unit was connected to a 1 m-long silicone tube and mounted outside of a side window of the vehicle. GEM concentrations in air were thus continuously quantified at 5 s intervals, by covering about 20 km of the coast by car at a speed of $\sim$20 km h^{-1}. This analyzer has been successfully used in various types of atmospheric mercury measurement campaign (e.g., Kim et al., 2006; Špirić and Mashyanov, 2000; Engle et al., 2006; Wang et al., 2006; Aiuppa et al., 2007; Muresan et al., 2007; Witt et al., 2008; Ci et al., 2011) where it was successfully used for continuous measurements of Hg distribution in the atmosphere over large city areas and various geological contexts both by walking traverse and from moving vehicles.

2.3. Mercury flux assessment at the sea–air interface

For the first time in this area, we used a plexiglass open-bottom dynamic flux chamber (emerged part: 50 × 50 × 50 cm; submerged part: 50 × 50 × 30 cm) technique coupled with a real-time atomic adsorption spectrometer (Lumex-RA 915+) to estimate the sea–air Hg evasion flux in the MBL (Fig. 2). The accumulation chamber was built by the technical staff working in the laboratories of electronic at IAMC-CNR (Capo Granitola), according to the different schemes proposed in literature (Kim and Lindberg, 1995; Carpi and Lindberg, 1998; Covelli et al., 1999; Wang et al., 2006). The Plexiglas was selected since it transmits all visible and UV wavelengths in solar radiation (89% and the 64% of UV-A and UV-B, respectively; Wang et al., 2006), which are responsible for the formation of photo-induced gaseous mercury in water. The floating chamber system was placed on the sea water surface with the edges of the chamber immersed 30 cm into the water to ensure a tight seal with the water, preventing entry of outside air. To homogenize the air inside the chamber two fans have been installed, suspended at about 5 cm from the top of the chamber. After positioning the chamber on the surface and achieving good contact, we were able to reach a steady-state of internal mercury concentration within approximately 10 min. This allowed us to reduce the flux chamber's influence on the environmental parameters of the sea water surface we were investigating, mainly wind speed and waves, because the chamber remains on the water for only a short period of time. Of course, this technique is suitable during relatively calm conditions of the sea, when the influence of these factors is negligible; anyway, the large size of the chamber reduces noise caused by the waves. Mercury flux from the water surface exposed in the chamber (0.25 m^2) was then calculated according to the Eq. (1) (Lindberg and Price, 1999; Zhang et al., 2001):

$$\Phi_{GEM} = Q(C_o - C_i)/A \tag{1}$$

where Φ_{GEM} is the GEM total emission rate per area and unit time (ng m^{-2} s^{-1}); $(C_o - C_i)$ is the difference in GEM concentrations in air exiting (C_o) and entering (C_i) the chamber (ΔC) (in ng m^{-3}); A is the basal area of the chamber in m^2; and Q is the flow rate of air flowing through the chamber in m^3 s^{-1}. Of course, the concentration differential used in the flux calculation must be greater than the system blank, which we determined based on the ΔC difference measured in the sunlight by sealing the chamber bottom to a large clean surface (a clear polycarbonate plate in our case). The QA/QC protocol of the experiment has been achieved in the field using
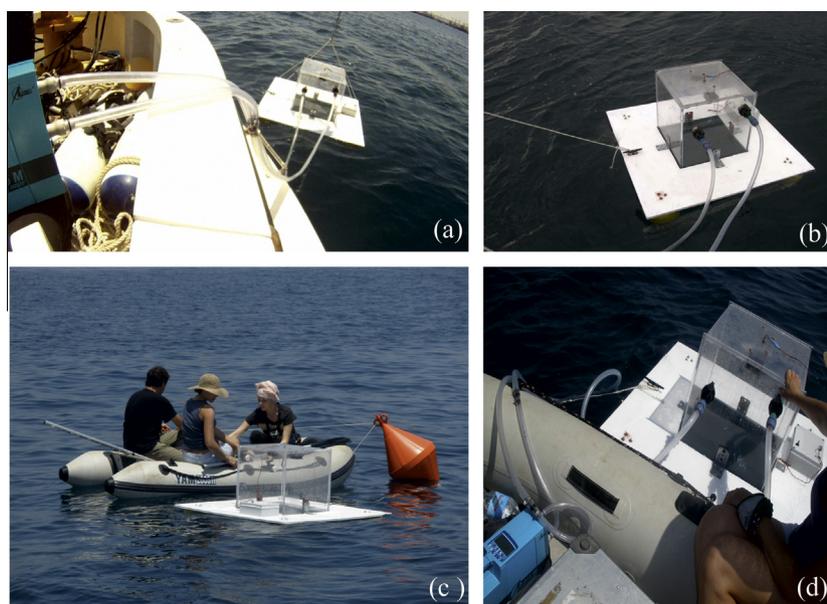

Fig. 2. Positioning (a-b), testing (c) and in real-time measurements (d) of sea–air GEM evasion flux by using the accumulation chamber technique.

blanks. Before and after each oceanographic cruise, the chamber was extensively cleaned with diluted laboratory detergent and several-fold rinsed with Milli-Q water. We find negligible blank value (GEM $_{blank}$ ~ 0.15 ng m^{-3}) which agrees well with the blank tests reported in literature (~0.2 ng GEM m^{-3}; Carpi and Lindberg, 1998; Gustin et al., 1999). The theoretical Hg concentration (from the manual calibration) has been compared to the measured concentration by direct injection into the analytical device and the recovery rate from direct injection into the flux chamber. The overall QA/QC protocol showed that up to 99% of the accuracy has been achieved by the technical protocol, as also confirmed by the low relative standard deviation exhibited by our data.

2.4. Bulk deposition collection

Bulk deposition was collected using a glass-made open collector (wet + dry deposition) according to Iverfeldt (1991) and Jensen and Iverfeldt (1994), which was located on the roof of the port authorities office close to downtown Augusta close to the weather station (Fig. 1a). Rainwater samples were collected at irregular intervals in function of the rainy events which affected the examined area. Samples were analyzed for total mercury concentrations (OSPAR, 1997) by a direct analyzer (Milestone DMA-80), which uses the principle of thermal decomposition, amalgamation and atomic absorption, in operation at IAMC-CNR (Capo Granitola). Before the analysis, each rainwater sample was weighed into a quartz boat, and transferred from the analytical balance to the DMA-80. Sample boats, loaded onto the instrument auto-sampler, are first dried and then thermally decomposed in a oxygen-rich furnace. Mercury and other combustion products are released from the sample and they are carried to the catalyst section of the furnace, where nitrogen and sulfur oxides, as well as halogens and other interfering compounds, are eliminated. Mercury is selectively trapped, in a separate furnace, through gold amalgamation. Combustion by-products are flushed off. The amalgamation furnace is heated and mercury is rapidly released. Mercury is flown via the carrier gas into a unique block with a tri-cell arrangement, positioned along the optical path of the spectrophotometer, where it is quantitatively measured by atomic absorption at 253.65 nm.

3. Results and discussions

3.1. Meterological pattern of the area

A meteorological data set, including wind direction, air temperature, and precipitation amount, was developed using data from the continuous acquisition by a weather station (DAVIS – Vantage Pro 2 Wi-Fi) installed on the roof of the Augusta port authorities office (Fig. 1a). Wind rose diagrams, median wind direction and dispersion parameters were computed by means of "openair" R statistical package. The overall (whole observation period) wind rose diagram (Fig. 3a) showed that the most frequent wind directions were related to NW and NE sectors. Winds from NW sector represents about the 50% of total observations, and were characterized by prevalent N-W direction (25%), while the prevalent one for NE sector (accounting for 35% of the total) was E-NE. We did not identify any relevant relation between the measured Hg concentrations in the MBL and meteorological parameters recorded during the survey.

3.2. GEM distribution in the MBL

The GEM measurements in the MBL over the Augusta basin have been performed along the same route in winter (November 2011) and summer (July 2011–June 2012) (Fig. 1b). During the sur-

vey, the wind speed ranged from 4.5 to 9.8 m s^{-1} and T_{air} from about 12–25 °C. During the cruises we measured averaged atmospheric GEM concentrations of ~1.5 ± 0.4 (range 0.9–3.1) and ~2.1 ± 0.98 (range 1.1–3.1) ng m^{-3} in the winter and summer, respectively (Table 1). The time-weighted average GEM concentrations show to some extent seasonal variations, as previously reported in literature for other geographic areas (Sprovieri et al., 2003; Sprovieri and Pirrone, 2008; Wangberg et al., 2008). Variability in our collected Hg data may be ascribed to the different intensity of the natural sunlight between winter and summer which represents a key parameter in controlling rates of % Hg^0 produced and then escaped from seawater surface (Costa and Liss, 1999); anyway the intensity of solar radiation has not been determined in this study. Time series evidence that collected data result somewhat higher than the atmospheric background Hg level measured over the land at the downtown urban site of Augusta (averaged 1.1 ± 0.3 ng m^{-3}; Table 1 and Fig. 4a), while are similar to those detected along the shore close to the dense industrial area surrounding the basin (range 1.5 ± 1.4–2 ± 1.6 ng m^{-3}), where we sporadically measured Hg peaks of about 8–10 ng m^{-3} (Fig. 4a). Estimated GEM at background levels suggests no significant acute toxicity since generally the lowest adverse effect observed has been fixed at 15–30 μg m^{-3} (~15–30 × 10^3 ng m^{-3}; Kazantzis, 2002). Anyway, GEM$_{atm}$ level over the Augusta basin results are to some extent higher than the background atmospheric mercury values reported for the North Hemisphere (range: 1.5–1.7 ng m^{-3}; Lindberg et al., 2007; evidenced by the dashed red lines in Fig. 4b), while are similar to those reported for a few polluted marine areas, like Tokyo Bay, the South China Sea and the Yellow Sea (1.9 ± 0.6, 2.8 ± 1.5 and 2.3 ± 0.7 ng m^{-3}, respectively; Narukawa et al., 2006; Fu et al., 2010; Ci et al., 2011; Table 1). Our data are also in the range proposed for many other oceans and seas, such as the Mediterranean (1.5 ± 0.3–2 ± 0.6 ng m^{-3}, Sprovieri et al., 2010) and the Adriatic Sea (1.6 ± 0.4 ng m^{-3}, Sprovieri and Pirrone, 2008), the Atlantic Ocean (1.3 ± 0.1–2 ± 0.1 ng m^{-3}, Temme et al., 2003) and the North Pacific Ocean (2.5 ± 0.5 ng m^{-3}, Laurier et al., 2003), while are higher than those measured over the equatorial Pacific Ocean (1.0 ± 0.1 ng m^{-3}, Kim and Fitzgerald, 1986) (Table 1). Finally, our data fit with results from the 2010 MED-OCEANOR cruise campaign recently performed by Fantozzi et al. (2013) in the Eastern Mediterranean (range: 1.3–1.8 ng GEM m^{-3}, averaged: 1.6 ± 0.1 ng m^{-3}; Table 1). By displaying data as a function of latitude (Fig. 5) and for comparison with the atmospheric total gaseous mercury (TGM = GEM + RGM) contents from other marine/oceanic environments (Kim and Fitzgerald, 1986; Slemr and Langer, 1992; Fitzgerald, 1995; Mason et al., 1998; Lamborg et al., 1999; Narukawa et al., 2006; Fu et al., 2010; Ci et al., 2011; Fantozzi et al., 2013) we found a small but discernible inter-hemispheric gradient in GEM resulting from greater emissions of Hg to the atmosphere in the more industrialized Northern Hemisphere. In compiling this diagram we considered that under the normal atmospheric condition, GEM is generally taken more than 95–98% among all the atmospheric Hg species (i.e. RGM and Hg$_p$; Ci et al., 2011). Since RGM is easily adsorbed by the seawater surface, most of the literature reported TGM measurements should be considered as GEM.

3.3. Air–sea GEM flux

Mercury leaves the ocean by evasion of dissolved Hg^0 when it is present at supersaturated concentration in the surface waters with respect to the atmosphere (Kim and Fitzgerald, 1986). Sea–air Hg evasion flux has been measured at seven monitoring stations selected along the Augusta basin (ST1-7; Fig. 1c and Table 2). During the oceanographic cruises, weather conditions were optimal, therefore the effect of wind, waves and presence of clouds were
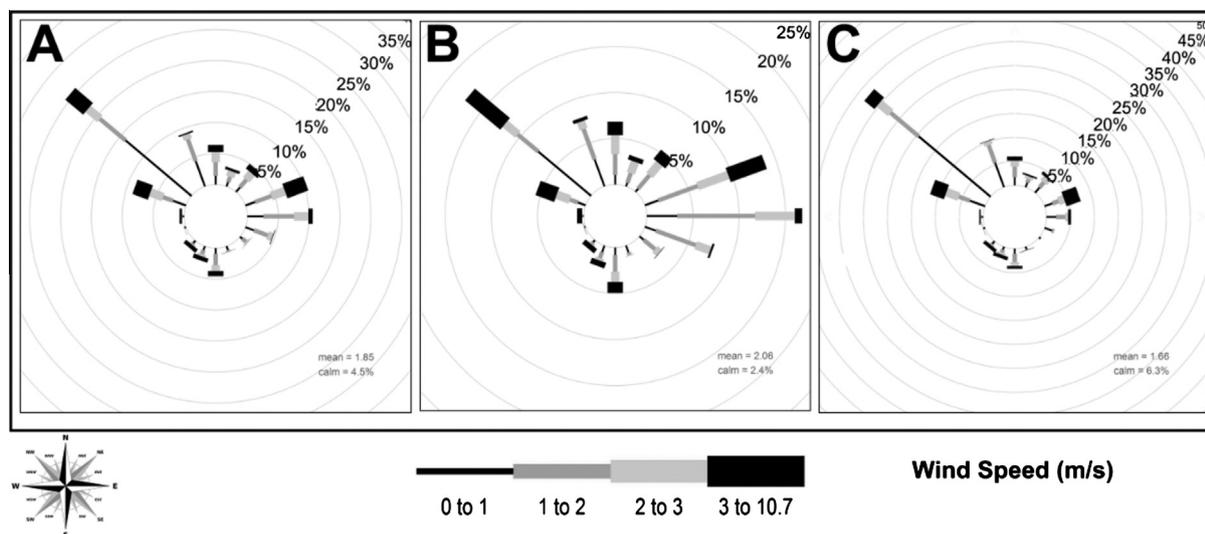
Fig. 3. Wind rose diagram built for the whole observation period showing the most frequent wind directions. Winds from NW sector represents about the 50% (c) of total observations, and were characterized by prevalent N-W direction (25%) (b), while the prevalent one for NE sector (accounting for 35% of the total) was E-NE (a).

Table 1
Gaseous elemental mercury (GEM) concentrations measured in the MBL over the Augusta basin compared to literature data for other acquatic environments. For a more detailed description on averages and methods the reader is referred to the original article.

Measurement sites	Period	GEM (ng m^{-3})		S.D. (n)	Methods	References
		Range	Mean			
Augusta Basin MBL						
Winter period averaged	2011/11/29–30	(0.9–3.1)	1.5	0.4 (8137)	Lumex RA-915 + analyzer	Present study
Summer period averaged	2011/07/11–12–2012/06/23–24	(1.1–3.1)	2.1	0.98 (159)	Lumex RA-915 + analyzer	Present study
Augusta downtown	11/11/2011	(0.8–1.4)	1.1	0.3 (129)	Lumex RA-915 + analyzer	Present study
Other sites						
Sweden coastal areas	October 1979–September 1980	(2.7–4)	3.4	0.4 (12)	Gold-traps	Brosset (1992)
North Atlantic ocean	October 1977–January 2000	(1.7–2)	2	0.1 (8)	Tekran 2537A analyzer	Temme et al. (2003)
South Atlantic ocean	October 1977–February 2001	(1–1.5)	1.3	0.1 (10)	Tekran 2537A analyzer	Temme et al. (2003)
South Atlantic	1996/05/20–1996/06/17	(1.2–1.9)	1.6	0.2 (14)	Gold-traps	Lamborg et al. (1999)
North pacific ocean	2002	(1.6–4.7)	2.5	0.5 (n.a.)	Tekran 2537A analyzer	Laurier et al. (2003)
Equatorial pacific ocean	1984/07/03–1984/06/08	(0.8–1.1)	1.0	0.008 (23)	Gold-traps	Kim and Fitzgerald (1986)
Indian ocean	2007	(1–1.5)	1.2	0.06 (n.a.)	Tekran 2537A analyzer	Witt et al. (2010)
Eastern Mediterranean sea	August 2003–September 2006	(1.3–2)	1.5	0.3 (5)	Tekran 2537A analyzer	Sprovieri et al. (2010)
Western Mediterranean	August 2003–July 2007	(1.2–2.7)	2	0.6 (3)	Tekran 2537A analyzer	Sprovieri et al. (2010)
East Mediterranean	2010/08/26–2010/09/13	(1.3–1.8)	1.6	0.1 (15)	Tekran 2537A analyzer	Fantozzi et al. (2013)
Baltic sea	1997/07/02–15	(1.4–2)	1.7	0.2 (11)	Tekran 2537A analyzer	Wängberg et al. (2001)
Baltic sea	1998/03/02–15	(1.2–1.6)	1.4	0.1 (9)	Tekran 2537A analyzer	Wängberg et al. (2001)
Adriatic sea	2004/10/26–2004/11/12	(0.8–3-3)	1.6	0.4 (n.a.)	Tekran 2537A analyzer	Sprovieri and Pirrone (2008)
Tokyo Bay	2003/12, 2004/10, 2005/01	(1.1–2.8)	1.9	0.6 (22)	Automated Hg analyzer	Narukawa et al. (2006)
South China sea	2008/05/09–2009/05/18	(1.5–4.5)	2.8	1.5 (n.a.)	Tekran 2537A analyzer	Fu et al. (2010)
Yellow sea	July 2007–May 2009	(1.12–7)	2.3	0.7 (1206)	Lumex RA-915 + analyzer	Ci et al. (2011)

n.a. = Not available.

not taken in consideration in discussing results. Our data range from 3.6 ± 0.3 (unpolluted site) to 72 ± 0.1 ng Hg m^{-2} h^{-1} (most polluted site) (Table 2), indicating that the sea–air evasion flux of Hg from the basin is not uniformly distributed but varies spatially (see Fig. 1c and Appendix I), while any particular trend across the two seasons (November 2011–June 2012) has been observed. Each flux value is devoid of the blank effect, since we subtracted the chamber blank value. The higher Hg evasion fluxes were estimated in the southern part of the basin (sampling stations ST1 and ST3, accounting for about 36 ± 0.3 and 72 ± 0.1 ng Hg m^{-2} h^{-1}, respectively; Fig. 1c), the most contaminated area of the basin in terms of Hg contained in the bottom sediments (0.1–527.3 mg Hg kg^{-1}, median value 23.8 mg Hg kg^{-1}; Sprovieri et al., 2011). On the other hand, the lowest Hg flux has been measured close to the northern sector of the basin (ST4, 3.6 ± 0.3 ng Hg m^{-2} h^{-1}; Table 2 and Fig. 1c), where the bottom sediments exhibited quite low Hg con-

tents (range: 0.1–12.7 mg kg^{-1}; median value 1.1 mg kg^{-1}; Sprovieri et al., 2011). These results suggest that the marine sediments are key contributors of Hg to the marine ecosystem and hence may represent a potential source of Hg to the atmosphere. By comparing our data with literature cases for many marine environments (Table 2), GEM$_{atm}$ flux over the Augusta basin resulted to be one order of magnitude higher than the averaged values reported for the Pacific Ocean (3 ± 2 ng m^{-2} h^{-1}; Kim and Fitzgerald, 1986), the Mediterranean Sea (2.2 ± 1.5 ng m^{-2} h^{-1}, Fantozzi et al., 2013; 2.5 ± 1.2 ng m^{-2} h^{-1}, Gardfeldt et al., 2003; 2.4 ± 1.5 ng m^{-2} h^{-1}, Ferrara et al., 2000), the Tyrrenian Sea (4.2 ± 3.2 ng m^{-2} h^{-1}, Gardfeldt et al., 2003; 1.6 ± 1.3 ng m^{-2} h^{-1}, Andersson et al., 2007), the Artic Ocean (2.4 ng m^{-2} h^{-1}, Andersson et al., 2008), the South China Sea (4.5 ± 3.4 ng m^{-2} h^{-1}, Fu et al., 2010), and the Tokyo Bay (5.8 ± 5 ng m^{-2} h^{-1}; Narukawa et al., 2006). In detail, our results are comparable both to the Hg flux
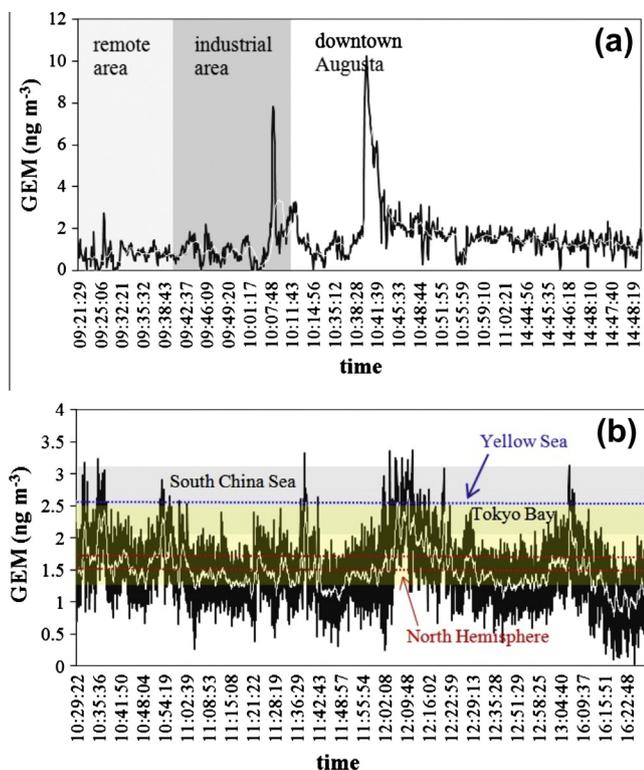
Fig. 4. Time series atmospheric GEM concentration measured (a) in the atmosphere over remote, industrial and urban areas close to the Augusta basin, and (b) at the MBL above the basin. (a) The atmospheric background Hg level measured over the land at the downtown urban site of Augusta is quite low (averaged 0.9 ± 0.5 ng m^{-3}), while we measured GEM concentrations peaks of about 8–10 ng m^{-3} along the coastline close to the dense industrial area surrounding the basin. (b) The yellow and grey areas indicate the concentration range of GEM measured over the Tokyo Bay (range: 1.3–2.5 ng m^{-3}) and the South China Sea (range: 2.1–3.1 ng m^{-3}), respectively, compiled by literature data (Narukawa et al., 2006; Fu et al., 2010). Blue dashed line indicates the averaged GEM value reported for the atmosphere over the polluted area of the Yellow Sea (Ci et al., 2011). Finally, our data result somewhat from similar to slightly higher than the range found at the North Hemisphere (red dashed lines; range: 1.5–1.7 ng m^{-3}; Lindberg et al., 2007). The simple moving average of our data (SMA) is also reported (white line) in both the graphs. (For interpretation of the references to colour in this figure legend, the reader is referred to the web version of this article.)
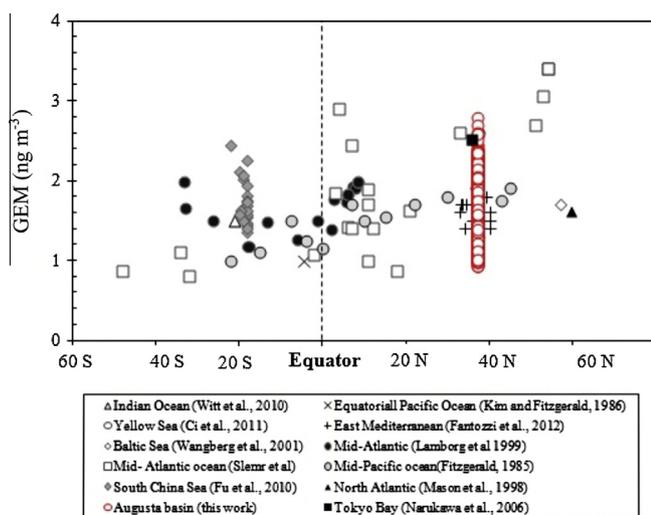

Fig. 5. Values for GEM found as a function of latitude over the Augusta basin. Also shown are compiled values for several marine/oceanic environmental systems (see text for the references).

value estimated over the Yellow Sea (3.2–44 ng m^{-2} h^{-1}; Ci et al., 2011) and the Atlantic Ocean (20–80 ng m^{-2} h^{-1}; Mason et al., 1998), this last containing extremely high dissolved gaseous mercury levels in waters. From Table 2 it emerges that most of the listed worldwide Hg sea/air evasion fluxes have been calculated indirectly by using the gas-exchange model (GEM; Liss and Slater, 1974); while only two data (plus the present study) refer to Hg flux values estimated by the dynamic flux chamber technique (DFC). The use of the dynamic flux chamber technique coupled with a real-time atomic adsorption spectrometer (Lumex-RA 915+) thus represents an important step aimed to refine the estimation method to assess Hg fluxes from environmental surfaces (Wang et al., 2006). This technique also aims to reduce the uncertainty in the goodness of processing data often given by the calculation model, strongly dependent from the choice of gas transfer parameterizations (Wanninkhof, 1992) and diffusion coefficient of mercury (Liss and Slater, 1974). To evaluate the impact of Hg emissions from different sources we must have a clear understanding of the factors controlling emissions, develop a data base of emissions from substrates with a wide range of Hg concentrations, and develop a framework for scaling point source measurements to broad areas. As listed in Table 2, our data, and more in general Hg evasion rates from acquatic environments, result to be higher than Hg flux from background uncontaminated soils ($\sim$0.9 ng Hg m^{-2} h^{-1}), while are comparable to those reported from volcanic/geothermal areas and substrates associated with hydrothermal systems ($\sim$14 and 83 ng Hg m^{-2} h^{-1}, respectively; Table 2). The highest Hg fluxes measured in areas of thermal activity are most likely due to a combination of diffuse Hg-bearing hydrothermal gas flow through soil and elevated Hg concentrations in thermal area substrates (Varekamp and Buseck, 1984). Finally, Hg flux measured at the sea/air interface in the Augusta Bay results to be several orders of magnitude lower than Hg released from areas associated with important ore deposits and metal mining, which are typically enriched in Hg relative to natural background concentrations (Table 2), and have averaged fluxes ranging from background rates (2 ng Hg m^{-2} h^{-1}) to tens of thousands of ng m^{-2} h^{-1} (3730–118000 ng Hg m^{-2} h^{-1}; Table 2). In order to calculate the total sea–air Hg evasion flux over the entire surface area of the Augusta basin (about 23.5 km^2), we used the model of territorial distribution proposed by Aurenhammer (1991) (the 'Voronoi Polygons' method). This method allowed us to split the basin in seven different areas (ST1-7, in km^2) each accounting for a different % of the total Hg evasion flux. Thus, we estimated a cumulative Hg evasion flux for the whole basin of about 0.004 t yr^{-1} ($\sim$9.7 $\pm$ 0.1 g d^{-1}), which accounts for $\sim$0.0002% of the global mercury oceanic evasion of 2000 t yr^{-1} proposed by Mason et al. (1994). Anyway, this value (9.7 $\pm$ 0.1 g d^{-1}) results to be lower than the total Hg flux emitted from the polluted Tokyo Bay (range 19–249 g d^{-1}; Sakata et al., 2006; Narukawa et al., 2006), but it is significant if we consider that the extent of the water surface area of the Augusta basin represents only a trivial % of the total oceanic surfaces on Earth (3.6×10^8 km^2; Eakins and Sharman, 2010) and 1/5 of the Tokyo Bay surface area (1000 km^2).

3.4. Bulk depositional flux assessment

Long-range transport of atmospheric gaseous Hg, followed by wet and dry deposition, is an important process by which Hg is supplied to terrestrial and aquatic ecosystems far from its source. Our preliminary data collected during a very short-term survey (from August 2011 to April 2012) (range: 21–32 ng L^{-1}; Appendix II) are comparable to those reported for rainwaters collected at the North Pacific Ocean (10–50 ng L^{-1}; Nishimura, 1979) and the North Sea (30 ng L^{-1}; Cambray et al., 1979). We also found a good correlation with Hg levels found in precipitations collected close to a chlorine caustic electrolysis plant (industrial area; 17 ng L^{-1}) and

Table 2
Mercury evasion flux from some acquatic environments reported in literature including this study. For a more detailed description on averages and methods the reader is referred to the original article.

Measurement sites	Date (year-month-day)	Hg(0) evasion flux (ng m^{-2} h^{-1}) Range	Mean (SD; n)	Methods	References
Augusta basin					
ST1	29/11/2011	(35.6–36.3)	36 (0.3; 2963)	DFC	Present study
ST2	29/11/2011	(14.2–14.5)	14.4 (0.1; 2965)	DFC	Present study
ST3	30/11/2011	(71.8–72.1)	72 (0.1; 2958)	DFC	Present study
ST4	29/11/2011	(3.2–3.9)	3.6 (0.3; 2963)	DFC	Present study
ST5	24/06/2012	(10.4–11.1)	10.8 (0.3; 2752)	DFC	Present study
ST6	23/06/2012	(7.1–7.3)	7.2 (0.1; 3244)	DFC	Present study
ST7	25/06/2012	(17.8–18.2)	18 (0.2; 4293)	DFC	Present study
Other acquatic sites					
Equatorial Pacific ocean	1984/07/03–1984/06/08	(0.5–8)	3 (2; 22)	GEM	Kim and Fitzgerald (1986)
Western Mediterranean	2003/08/20–23	(4.1–6.2)	5.1 (1; 275)	GEM	Andersson et al. (2007)
Western Mediterranean	2000/07/14–2000/08/09	(0.5–4.5)	2.5 (1.2; 6)	GEM	Gardfeldt et al. (2003)
Eastern Mediterranean	2000/07/17–23	(1.6–15.2)	7.9 (4.2; 10)	GEM	Gardfeldt et al. (2003)
Eastern Mediterranean	2010/08/26–2010/09/13	(0.2–4.9)	2.2 (1.5; 17)	GEM	Fantozzi et al. (2013)
Mediterranean Sea	1998/02/06–1998/09/22	(1.2–5.7)	2.4 (1.5; 6)	DFC	Ferrara et al. (2000)
Tyrrenian sea	2003/08/27–2004/10/29	(0.4–4.1)	1.6 (1.3; 675)	GEM	Andersson et al. (2007)
Tyrrenian sea	2000/07/29–2000/08/08	(0.1–9.9)	4.2 (3.2; 7)	GEM	Gardfeldt et al. (2003)
Ionian sea	2003/08/08–2004/11/11	(0.8–6.6)	2.7 (1.8; 888)	GEM	Andersson et al. (2007)
Adriatic sea	2004/11/02–10	(2–9.7)	5.4 (2.5; 401)	GEM	Andersson et al. (2007)
North Adriatic sea	2004/11/05–06	(23.7–33.2)	28.4 (4.7; 104)	GEM	Andersson et al. (2007)
Strait of Sicily	2003/08/06–2004/03/26	(0.7–3.5)	2.1 (1.4; 329)	GEM	Andersson et al. (2007)
Mediterranean coastal water	2000/07/31–2000/08/07	(2.7–4.5)	3.7 (0.8; 63)	DFC	Gardfeldt et al. (2003)
North Atlantic Ocean	2005/07/07–11	(−0.6 to 2.5)	0.4 (0.3; 559)	GEM	Andersson et al. (2011)
Baltic sea	1997/07/02–15	(6–89)	31 (25; 11)	GEM	Wängberg et al. (2001)
Artic ocean	2005/07/13–2005/09/25	(n.a.)	2.4 (n.a.)	GEM	Andersson et al. (2008)
North sea	1992/09/n.a.	(2.4–46)	20 (13; 11)	GEM	Baeyens and Leermakers (1998)
South China Sea	2007/08/11–27	(0.2–15.3)	4.5 (3.4; 40)	GEM	Fu et al. (2010)
Tokyo Bay	2003/12/10–2005/01/12	(0.1–22)	5.8 (5; 22)	GEM	Narukawa et al. (2006)
Yellow sea	2010/07/10–17	(3.2–44)	18.3 (11.8; 40)	GEM	Ci et al. (2011)
Land evasion					
Background unpolluted soils (US)	n.a.	(0.3–0.8)	0.9 (0.2; 1326)	DFC	Ericksen et al. (2006)
Volcanic/geothermal areas (LVC)	2000/04/14–15	(5.2–19.8)	13.7 (8; 12)	DFC	Engle and Gustin (2002)
Mineralized area (Peavine peak, Nevada)	2000/04/14–15	(2–15)	10 (n.a.; 16)	DFC	Engle and Gustin (2002)
Mine-waste enriched soils (Mt. Amiata)	2008/08/27–28	(250–8000)	3730 (n.a.; 56)	DFC	Fantozzi et al. (2013), in press
Gold Mines (Venezuela)	2004/05/16–31	(650–420100)	118000 (n.a.; 12)	DFC	García-Sanchez et al. (2006)
Hydrothermal systems (Lassen Park)	2004/08/20–21	(-110 to 103)	12 (n.a.; 13)	DFC	Engle et al. (2006)
Hydrothermal systems (Yellowstone)	2003/09/12–2004/09/01	(-27 to 541)	83 (n.a.; 106)	DFC	Engle et al. (2006)
Sulfur Bank geothermal area	n.a.	(436–510)	n.a (n.a.)	DFC	Gustin (2003)

DFC = dynamic flux chamber; GEM = gas-exchange model; n.a. = not available.

to the mineralized area of Mt. Amiata (Cinnabar deposits) near vapor-dominated geothermal springs (14.4 ng L^{-1}) (Ferrara et al., 1986). By attempting to calculate a first Hg bulk depositional flux (wet + dry) for the Augusta basin, we used the following relation:

$$\Phi_{Hg} = (C_{Hg} \cdot P)T^{-1} \quad (2)$$

where C_{Hg} is the concentration of Hg in rain (in ng L^{-1}), P is the amount of precipitation (in mm), and T is the exposition time of the collector (in days). We estimated a preliminary Hg bulk depositional flux ranging from 0.05 to 0.23 µg m^{-2} d^{-1} (weighted average of 0.10 µg m^{-2} d^{-1}; Appendix II). Although our estimated average Hg bulk deposition flux (35.8 µg m^{-2} yr^{-1}) at the Augusta basin is higher than the values calculated by Mason et al. (1994) to ocean (from 0.13 to 9.5 µg m^{-2} yr^{-1}) and land (0.1–19.8 µg m^{-2} yr^{-1}) at various latitudes (Downs et al., 1998), it results to be one order of magnitude lower than the annually atmospheric Hg flux released in the MBL (maximum emission ~315 µg m^{-2} yr^{-1}; this work).

4. Conclusions

Mercury has an extremely complex cycle in the Earth's ecosystems and the environmental bodies are both active sink and source for Hg. The exchange of mercury between natural surfaces and the atmosphere is an important process for the atmospheric cycling and environmental turnover of this element. The new data set proposed in this study offers a unique and original opportunity to study the potential outflow of Hg from the sea–air interface at the Augusta basin, and will serve as a basis for future estimates on Hg mass balance in this area.

Appendix A. Supplementary data

Supplementary data associated with this article can be found, in the online version, at http://dx.doi.org/10.1016/j.chemosphere.2013.07.025.

References

Aiuppa, A., Bagnato, E., Witt, M.L.I., Mather, T.A., Parello, F., Pyle, D.M., Martin, R.S., 2007. Real-time simultaneous detection of volcanic Hg and SO$_2$ at La Fossa Crater, Vulcano (Aeolian Islands, Sicily). Geophysical Research Letters 34, L21307. http://dx.doi.org/10.1029/2007GL030762.

Amos, H.M., Jacob, D.J., Holmes, C.D., Fisher, J.A., Wang, Q., Yantosca, R.M., Corbitt, E.S., Galarneau, E., Rutter, A.P., Gustin, M.S., Steffen, A., Schauer, J.J., Graydon, J.A., St. Louis, V.L., Talbot, R.W., Edgerton, E.S., Zhang, Y., Sunderland, E.M., 2012. Gas-particle partitioning of atmospheric Hg(II) and its effect on global mercury deposition. Atmospheric Chemistry and Physics 12, 591–603.

Andersson, M.E., Gårdfeldt, K., Wängberg, I., Sprovieri, F., Pirrone, N., Lindqvist, O., 2007. Seasonal and daily variation of mercury evasion at coastal and off shore sites from the Mediterranean Sea. Marine Chemistry 104, 214–226.

Andersson, M.E., Sommar, J., Gardfeldt, K., Lindqvist, O., 2008. Enhanced concentrations of dissolved gaseous mercury in the surface waters of the Arctic Ocean. Marine Chemistry 110, 190–194.

Andersson, M.E., Sommar, J., Gårdfeldt, K., Jutterström, S., 2011. Air–sea exchange of volatile mercury in the North Atlantic Ocean. Marine Chemistry 125, 1–7.

Aurenhammer, F., 1991. Voronoi diagrams—a survey of a fundamental geometric data structure. ACM Computing Surveys 23 (3), 345–405.

Baeyens, W., Leermakers, M., 1998. Elemental mercury concentrations and formation rates in the Scheldt estuary and the North Sea. Marine Chemistry 60, 257–266.

Bothner, M.H., Jahnke, R.A., Peterson, M.L., Carpenter, R., 1980. Rate of loss from contaminated estuarine sediments. Geochimica et Cosmochimica Acta 44, 273–285.

Brosset, C., 1992. Total airborn mercury and its possible origin. Water, Air and Soil Pollution 17, 37–50.

Cambray, R.S., Jeffries, D.F., Topping, G., 1979. The atmospheric input of trace elements to the North Sea. Marine Science Communications 5, 175–194.

Carpi, A., Lindberg, S.E., 1998. Application of a Teflon (TM) dynamic flux chamber for quantifying soil mercury flux: tests and results over background soil. Atmospheric Environment 32 (5), 873–882.

Ci, Z.J., Zhang, X.S., Wang, Z.W., Niu, Z.C., Diao, X.Y., Wang, S.W., 2011. Distribution and air–sea exchange of mercury (Hg) in the Yellow Sea. Atmospheric Chemistry and Physics 11, 2881–2892. http://dx.doi.org/10.5194/acp-11-2881-2011.

Costa, M., Liss, P.S., 1999. Photoreduction of mercury in seawater and its possible implication for Hg0 air–sea fluxes. Marine Chemistry 68, 87–95.

Covelli, S., Faganeli, J., Horvat, M., Brambati, A., 1999. Porewater distribution and benthic flux measurements of mercury and methylmercury in the gulf of trieste (Northern Adriatic Sea). Estuarine, Coastal and Shelf Science 48, 415–428.

Downs, S.G., MacLeod, C.L., Lester, J.N., 1998. Mercury in precipitation and its relation to bioaccumulation in fish: a literature review. Water Air and Soil Pollution 108, 149–187.

Eakins, B.W., Sharman, G.F., 2010. Volumes of the World's Oceans from ETOPO1. NOAA National Geophysical Data Center, Boulder, CO. 2010.

Engle, M.A., Gustin, M.S., 2002. Scaling of atmospheric mercury emissions from three naturally enriched areas: Flowery Peak, Nevada; Peavine Peak, Nevada; and Long Valley Caldera, California. The Science of the Total Environment 290, 91–104.

Engle, M.A., Gustin, M.S., Goff, F., Counce, D.A., Janik, C.J., Bergfeld, D., Rytuba, J.J., 2006. Atmospheric mercury emissions from substrates and fumaroles associated with three hydrothermal systems in the western United States. Journal of Geophysical Research 111, D17304. http://dx.doi.org/10.1029/2005JD006563.

Ericksen, J.A., Gustin, M.S., Xin, M., Weisberg, P.J., Fernandez, G.C.J., 2006. Air–soil exchange of mercury from background soils in the United States. Science of The Total Environment 366 (2–3), 851–863.

Ericksen, J.A., Gustin, M.S., Lindberg, S.E., Olund, S.D., Krabbenhoft, D.P., 2005. Assessing the potential for re-emission of mercury deposited in precipitation from arid soils using a stable isotope. Environmental Science Technology 39, 8001–8007.

Fantozzi, L., Manca, G., Ammoscato, I., Pirrone, N., Sprovieri, F., 2013. The cycling and sea–air exchange of mercury in the waters of the Eastern Mediterranean during the 2010 MED-OCEANOR cruise campaign. Science of the Total Environment 448, 151–162.

Ferrara, R., Maserti, B., Petrosino, A., Bargagli, R., 1986. Mercury levels in rain and air and the subsequent washout mechanism in a central Italian region. Atmospheric Environment 20 (1), 125–128.

Ferrara, R., Mazzolai, B., Lanzillotta, E., Nucaro, E., Pirrone, N., 2000. Temporal trends in gaseous mercury evasion from the Mediterranean Seawaters. Science of the Total Environment 259, 183–190.

Fitzgerald, W.F., 1995. Is mercury increasing in the atmosphere? The need for an atmospheric mercury network (AMNET). Water Air and Soil Pollution 28, 245–254. http://dx.doi.org/10.1007/BF01189674.

Fu, X., Feng, X., Zhang, G., Xu, W., Li, X., Yao, H., Liang, P., Li, J., Sommar, J., Yin, R., Liu, N., 2010. Mercury in the marine boundary layer and seawater of the South China Sea: concentrations, sea/air flux, and implication for land outflow. Journal of Geophysical Research 115, D06303. http://dx.doi.org/10.1029/2009JD012958, 2010.

García-Sanchez, A., Contreras, F., Adams, M., Santos, F., 2006. Atmospheric mercury emissions from polluted gold mining areas (Venezuela). Environ Geochem Health 28, 529–540.

Gardfeldt, K., Sommar, J., Ferrara, R., Ceccarini, C., Lanzillotta, E., Munthe, J., Wangberg, I., Lindqvist, O., Pirrone, N., Sprovieri, F., Pesentid, E., Stromberg, D., 2003. Atmospheric Environment 37, S73–S84.

Gustin, M.S., 2003. Are mercury emissions from geologic sources significant? A status report. The Science of the Total Environment 304, 153–167.

Gustin, M.S., Lindberg, S., Marsik, F., Casimir, A., Ebinghaus, R., Edwards, G., et al., 1999. Nevada STORMS project: measurement of mercury emissions from naturally enriched surfaces. Journal of Geophysical Research Atmosphere 104 (21), 831–844.

ICRAM,2005. (Istituto Centrale Per La Ricerca Scientifica E Tecnologica Applicata Al Mare), elaborazione e valutazione dei risultati della caratterizzazione ambientale della Rada di Augusta—aree prioritarie ai fini della progettazione degli interventi di messa in sicurezza di emergenza—Sito di interesse nazionale di Priolo, BoI-Pr-SI-PR-Rada di Augusta-01.04, 2005, 92.

Iverfeldt, A., 1991. Mercury in the forest canopy throughfall water and its relation to atmospheric deposition. Water Air and Soil pollution 56, 553–564.

Jensen, S., Iverfeldt, Å., 1994. Atmospheric bulk deposition of mercury to the southern Baltic Sea Area. In: Watras, C.J., Huckabee, J.W. (Eds.), Mercury Pollution: Integration and Synthesis. Lewis Publishers, Boca Raton, FL, USA, pp. 221–230.

Kazantzis, G., 2002. Mercury exposure and early effects: an overview. La Medicina del Lavoro 93 (3), 139–147.

Kim, J.P., Fitzgerald, W.F., 1986. Sea-air partitioning of mercury in the equatorial Pacific Ocean. Science 231, 311–330.

Kim, K.H., Lindberg, S., 1995. Design and initial tests of dynamic enclosure chamber for measurements of vapour-phase mercury fluxes over soils. Water, Air and Soil Pollution 80, 1059–1068.

Kim, K.H., Ebinghaus, R., Schroeder, W.H., Blanchard, P., Kock, H.H., Steffen, A., Froude, F.A., Kim, M.J., Hong, S., Kim, J.H., 2005. Atmospheric mercury concentrations from several observatory sites in the Northern Hemisphere. Journal of Atmospheric Chemistry 50 (1), 1–24.

Lamborg, C.H., Rolfhus, K.R., Fitzgerald, W.F., Kim, G., 1999. The atmospheric cycling and air–sea exchange of mercury species in the South and equatorial Atlantic Ocean. Deep-Sea Research II 46, 957–977.

Lamborg, C.H., Fitzgerald, W.F., O'Donnell, J., Torgersen, T., 2002. A non-steady-state compartmental model of global-scale mercury biogeochemistry with inter-hemispheric atmospheric gradients. Geochimica et Cosmochimica Acta 66 (7), 1105–1118.

Laurier, F.J.G., Mason, R.P., Whalin, L., 2003. Reactive gaseous mercury formation in the North Pacific Ocean's marine boundary layer: a potential role of halogen chemistry. Journal of Geophysical Research 108 (D17), 4529. http://dx.doi.org/10.1029/2003JD003625.

Le Donne, K., Ciafani, S., 2008. Monitoraggio dell'inquinamento atmosferico da mercurio nei principali impianti cloro-soda italiani. Ingegneria Ambientale 37, 45–52.

Lindberg, S.E., Price, J.L., 1999. Airborne emissions of mercury from municipal land. II. Operations: a short-term measurement study in Florida. Journal of Air Waste Management Association 49, 520–532.

Lindberg, S., Bullock, R., Ebinghaus, R., Daniel, E., Feng, X., Fitzgerald, W., Pirrone, N., Prestbo, E., Seigneur, C., 2007. A synthesis of progress and uncertainties in attributing the sources of mercury in deposition. Ambio 36 (1), 19–32.

Liss, P.S., Slater, P.G., 1974. Flux of gases across the air–sea interface. Nature 247, 181–184.

Mason, R.P., Fitzgerald, W.F., Morel, F.M.M., 1994. The biogeochemical cycling of elemental mercury. Geochimica et Cosmochimica Acta 58 (15), 3191–3198.

Mason, R.P., Rolfhus, K.R., Fitzgerald, W.F., 1998. Mercury in the North Atlantic. Marine Chemistry 61, 37–53.

Muresan, B., Cossa, D., Jézéquel, D., Prévot, F., Kerbellec, S., 2007. The biogeochemistry of mercury at the sediment water interface in the Thau lagoon. 1. Partition and speciation. Estuarine, Coastal and Shelf Science 72 (3), 472–484.

Narukawa, M., Sakata, M., Marumoto, K., Asakura, K., 2006. Air–sea exchange of mercury in Tokyo Bay. Journal of Oceanography 62, 249–257.

Nishimura, M., 1979. Determination of mercury in the aquatic environment and its global movements. ACS/CSJ Chemical Congress INOR 175. Honolulu, Hawaii.

OSPAR, 1997. JAMP Guidelines for the sampling and analysis of mercury in air and precipitation. OSPAR Commision, Monitor guideline Ref. n. 1997–8. London.

Pacyna, J.M., Pacyna, P.E., 1998. Global Emissions of Mercury to the Atmosphere: Emissions from Anthropogenic Sources. Norwegian Institute for Air Research (NILU), Kjeller, Norway, Draft Report. Version 1.2.

Rajar, R., Cetina, M., Horvat, M., Zagar, D., 2007. Mass balance of mercury in the Mediterranean Sea. Marine Chemistry 107, 89–102.

Sakata, M., Marumoto, K., Narukawa, M., Asakura, K., 2006. Regional variations in wet and dry deposition fluxes of trace elements in Japan. Atmospheric Environment 40, 521–531.

Schroeder, W.H., Munthe, J., 1998. Atmospheric mercury-an overview. Atmospheric Environment 809–822 (97), 00293–00298. http://dx.doi.org/10.1016/S1352-2310.

Sholupov, S., Pogarev, S., Ryzhov, V., Mashyanov, N., Stroganov, A., 2004. Zeeman atomic absorption spectrometer RA–915+ for direct determination of mercury in air and complex matrix Samples. Fuel Processing Technology 85 (473–485), 2004.

Slemr, F., Langer, E., 1992. Increase in global atmospheric concentrations of mercury inferred from measurements over the Atlantic Ocean. Nature 355, 434–436.

Špiric, Z., Mashyanov, N.R., 2000. Mercury measurements in ambient air near natural gas processing facilities. Fresenius Journal of Analytical Chemistry 366 (5), 429–432.

Sprovieri, F., Pirrone, N., 2008. Spatial and temporal distribution of atmospheric mercury species over the Adriatic Sea. Environmental Fluid Mechanics 8, 117–128.

Sprovieri, F., Pirrone, N., Gardfeldt, K., Sommar, J., 2003. Mercury speciation in the Marine Boundary Layer along a 6000 km cruise path around the Mediterranean Sea. Atmospheric Environment 37, 63–71.

Sprovieri, F., Hedgecock, I.M., Pirrone, N., 2010. An investigation of the origins of reactive gaseous mercury in the Mediterranean marine boundary layer. Atmospheric Chemistry and Physics 10, 3985–3997. http://dx.doi.org/10.5194/acp-10-3985-2010, 2010.

Sprovieri, M., Oliveri, E., Di Leonardo, R., Romano, E., Ausili, A., Gabellini, M., et al., 2011. The key role played by the Augusta basin (southern Italy) in the mercury contamination of the Mediterranean Sea. Journal of Environmental Monitoring 13, 1753–1760.

Temme, C., Slemr, F., Ebinghaus, R., Einax, J.W., 2003. Distribution of mercury over the Atlantic Ocean in 1996 and 1999–2001. Atmospheric Environment 37, 1889–1897.

Travnikov, O., 2005. Contribution of the intercontinental atmospheric transport to mercury pollution in the Northern Hemisphere. Atmospheric Environment 39 (39), 7541–7548.

Varekamp, J.C., Buseck, P.R., 1984. The speciation of mercury in hydrothermal systems, with applications for ore deposition. Geochimica et Cosmochimica Acta 48, 177–186.

Wang, D., He, L., Shi, X., Wei, S., Feng, X., 2006. Release flux of mercury from different environmental surfaces in Chongqing, China. Chemosphere 64, 1845–1854.

Wängberg, I., Schmolke, S., Schager, P., Munthe, J., Ebinghaus, R., Iverfeldt, Å., 2001. Estimates of air–sea exchange of mercury in the Baltic Sea. Atmospheric Environment 28, 5477–5484. http://dx.doi.org/10.1016/S1352-2310(01)00246-1.

Wangberg, I., Munthe, J., Amouroux, D., Andersson, M., Fajon, V., Ferrara, R., Gardfeldt, K., Horvat, M., Mamane, Y., Melamed, E., Monperrus, M., Ogrinc, N., Yossef, O., Pirrone, N., Sommar, J., Sprovieri, F., 2008. Atmospheric mercury at mediterranean coastal stations. Environmental Fluid Mechanics 8, 101–116. http://dx.doi.org/10.1007/s10652-007-9047-2.

Wanninkhof, R., 1992. Relationship between windspeed and gas exchange over the ocean. Journal of Geophysical Research 97, 7373–7382.

Witt, M.L.I., Mather, T.A., Pyle, D.M., Aiuppa, A., Bagnato, E., Tsanev, V.I., 2008. Mercury and halogen emissions from Masaya and Telica volcanoes, Nicaragua. Journal of Geophysical Research 113, B06203. http://dx.doi.org/10.1029/2007JB005401.

Witt, M.L.I., Mather, T.A., Baker, A.R., De Hoog, J.C.M., David, M.P., 2010. Atmospheric trace metals over the south-west Indian Ocean: total gaseous mercury, aerosol trace metal concentrations and lead isotope ratios. Marine Chemistry 121, 2–16.

Zhang, H., Lindberg, Steve.E., Marsik, F.J., 2001. Mercury air/surface exchange kinetics of background soils of the Tahquamenon river in the Michigan upper peninsula. Water Air Soil Pollution 126, 151–169.